

Patterns and mechanisms of repeat drainages of glacier-dammed Dañ Zhùr (Donjek) Lake, Yukon

Moya Painter^a, Luke Copland^b, Christine Dow^b, Will Kochtitzky^{b,a,c}, and Dorota Medrzycka^b

^aDepartment of Geography, Environment and Geomatics, University of Ottawa, Ottawa, ON K1N 6N5, Canada; ^bDepartment of Geography and Environmental Management, University of Waterloo, 200 University Avenue W., Waterloo, ON N2L 3G1, Canada;

^cSchool of Marine and Environmental Programs, University of New England, Biddeford, ME 04005, USA

Corresponding author: **Luke Copland** (email: luke.copland@uottawa.ca)

Abstract

Dañ Zhùr (Donjek) Glacier is a surge-type glacier that undergoes cyclical periods of rapid advance over ~1–2 years, followed by retreat for ~10 years. Since the 1990s, the advances have caused the formation of ice-dammed Dañ Zhùr Lake, which has filled and drained in summers following a surge event. Here, we report how these drainages initially occur through a subglacial channel under the glacier terminus, which then typically closes the following winter, enabling another lake to form and drain the next summer. However, our remote sensing and field observations indicate that after several drainage events, a subaerial ice canyon is formed through the glacier terminus, which prevents another lake from forming until after the glacier surges again. We predict that the next surge of Dañ Zhùr Glacier will occur around the mid-2020s, causing the formation of a larger Dañ Zhùr Lake during the following quiescent phase because, despite periodic advances, a long-term trend of glacier recession is exposing a larger basin for the lake to form in. However, each subsequent surge is causing less terminus advance than the previous one, until ultimately the surges will be insufficient to dam Dañ Zhùr Chù' (Donjek River), and lakes will cease to form.

Key words: glacier surge, glacier lake outburst flood, ice-dammed lake, ice hazard

1. Introduction

Glacier-dammed lakes form when a glacier or moraine blocks the flow of water. Glacial lake outburst floods (GLOFs) can occur when the dam fails, leading to the sudden release of water and flash flooding (Clague and O'Connor 2015). These lakes can occur anywhere glaciers are present, and these floods are one of the most common glacier hazards (Hock et al. 2019). A recent global assessment of hazards posed by GLOFs indicates that the number and area of glacial lakes has grown rapidly since 1990 (Taylor et al. 2023), with these trends expected to continue in the coming decades to century as glaciers recede in a warming climate (Harrison et al. 2018; Hock et al. 2019). In Alaska and NW Canada, Rick et al. (2022) report that the total area of ice marginal lakes grew by 59% (483 km²) between 1984–1988 and 2016–2019, although there was a marked difference between a reduction in area of ice-dammed lakes (–40%) and increase in area of moraine-dammed lakes (+87%) over this period.

There are many trigger mechanisms that cause a glacier or moraine dam to fail, some of which can cause sudden drainage events. Overspilling occurs when the water level exceeds the height of the dam and is more common for cold-based glaciers that are frozen to the bed (Maag 1972), or when a rockslide, avalanche, or ice fall hits the lake (Somos-Valenzuela et al. 2016). Flotation of a glacier dam can occur

when the lake water column reaches a height of ~90% of the adjacent ice thickness (Knight and Russell 1993; Björnsson 2009). Dam flotation can be a cyclical event, with water draining during flotation and then becoming dammed again once the lake reaches a lower level (Iturrizaga 2011). Subaerial breach-widening occurs when there is a sudden rupture or detachment of the glacier or moraine dam (Walder and Costa 1996). Volcanic and seismic activity can also trigger a GLOF, which is common in locations such as Iceland (Björnsson 1992; Jóhannesson 2002).

A common process that can lead to the formation of a glacier-dammed lake is when an advancing glacier enters a river valley. Given that nearly all glaciers globally are retreating (Zemp et al. 2015), surging is one of the few mechanisms by which glaciers currently advance. Southwest Yukon and Alaska are home to numerous surge-type glaciers (Sevestre and Benn 2015), many of which intersect river valleys at angles conducive to damming. Several ice-dammed lakes have been previously formed, and subsequently drained, at the termini of surge-type glaciers in Yukon. For example, Nàtùdäy (Lowell) Glacier repeatedly blocked the Alsek River during surges prior to the late 1800s (Clague and Rampton 1982), creating an ice-dammed lake up to 200 m deep, altering salmon migration routes, and resulting in death and destruction in downstream communities when the ice dam broke (Cruikshank 2001). Repeated surges of Steele Glacier created

Hazard Lake, which has rapidly drained subglacially several times in the past decades (Clarke 1982).

At Dañ Zhùr (Donjek) Glacier, ice-dammed lakes have been formed and drained numerous times during at least the last thousand years (Perchanok 1980). Kochtitzky et al. (2019) reported that Dañ Zhùr Glacier has surged eight times since the 1930s, with recent surges resulting in the full or partial damming of Dañ Zhùr Chù' (Donjek River), the formation of an ice marginal lake, and most lakes draining through an outburst flood (Kochtitzky et al. 2020). However, little is currently known about the processes that control the outburst floods at Dañ Zhùr Glacier, whether they are changing over time, and whether they have resulted in significant risk or disturbance to downstream areas. Examining these issues is relevant not only for Dañ Zhùr Glacier, but also for other glaciers in the region that either currently have temporally varying glacial lakes or may form them in the future. Here, we document the patterns and mechanisms of the drainage of ice-dammed Dañ Zhùr Lake, with a focus on the most recent drainage event in 2019 when we have field observations to complement the satellite remote sensing record to examine how the lake drains and the implications of this event for downstream regions.

2. Study area

Dañ Zhùr Glacier (61°12'40''N, 139°30'50''W) flows from the eastern side of the St. Elias Mountains, southwest Yukon, Canada (Fig. 1). The glacier is 65 km long and covered an area of 448 km² in 2010, with the terminus at ~1000 m above sea level (a.s.l.) and the accumulation area extending to >3000 m a.s.l. (Kochtitzky et al. 2020). Dañ Zhùr Glacier has surged approximately every 12 years since at least the 1930s, with eight documented surge events in ~1935, ~1947, late 1950s, ~1969, 1977–79, 1988–1990, 2000–2002, and 2012–2014 (Abe et al. 2016; Kochtitzky et al. 2019). Since the Little Ice Age, Dañ Zhùr Glacier has retreated by an average of ~2.5 km, with each surge typically reaching a lesser extent than the one before it (Kochtitzky et al. 2019; Fig. 1).

Dañ Zhùr Chù' valley has received significant attention in recent decades as the location of potential flooding risk because Dañ Zhùr Glacier enters the main valley approximately perpendicularly. This orientation creates a mechanism for damming the river and creating an ice marginal lake (or lakes) during or after a surge, which can drain catastrophically when the glacier retreats. We refer to such lakes as Dañ Zhùr Lake, with Kochtitzky et al. (2020) finding that their area has been increasing since 2001, and that their drainage is occurring sooner after surge termination than those before. This recent increase in lake size has occurred because the retreating glacier has left behind a basin of increasing size between the terminus and a Neoglacial terminal moraine in which ice-dammed lakes are able to form.

As we describe in detail in the following sections, Dañ Zhùr Lake has drained either partially or fully at least seven times since the 1990s, many of which have caused an outburst flood (Kochtitzky et al. 2020). Surges of Dañ Zhùr Glacier between the 1930s and 1980s were more extensive, but there is little evidence that large ice marginal lakes occurred during

this time due to the lack of a basin for them to form in (Kochtitzky et al. 2020). However, geomorphological evidence suggests that ice-dammed lakes have been present at the terminus of Dañ Zhùr Glacier as early as 1270, with numerous drainage events over the centuries (Perchanok 1980). The occurrence of historical flood events is supported by modelling by Clarke and Mathews (1981), which suggests that a large blockage of the river during past centuries could create a lake with a volume of 0.234 km³, with a potential maximum peak discharge rate of 5968 m³ s⁻¹ during drainage. While such a large event is unlikely to occur given the recent retreat of Dañ Zhùr Glacier (Kochtitzky et al. 2019), future surge events can still create ice-dammed lakes.

Past drainage events have impacted the people inhabiting the region, with Chief Albert Isaac describing an incident downstream of Dañ Zhùr Glacier that occurred during his lifetime where one man was killed by an “explosion of ice” while crossing the river (Cruikshank 2005). The area surrounding Dañ Zhùr Glacier is sparsely populated, but the Alaska Highway crosses the Dañ Zhùr Chù' ~50 km downstream and is well traveled year-round by residents and tourists as it is the only road in the region linking many communities.

3. Materials and methods

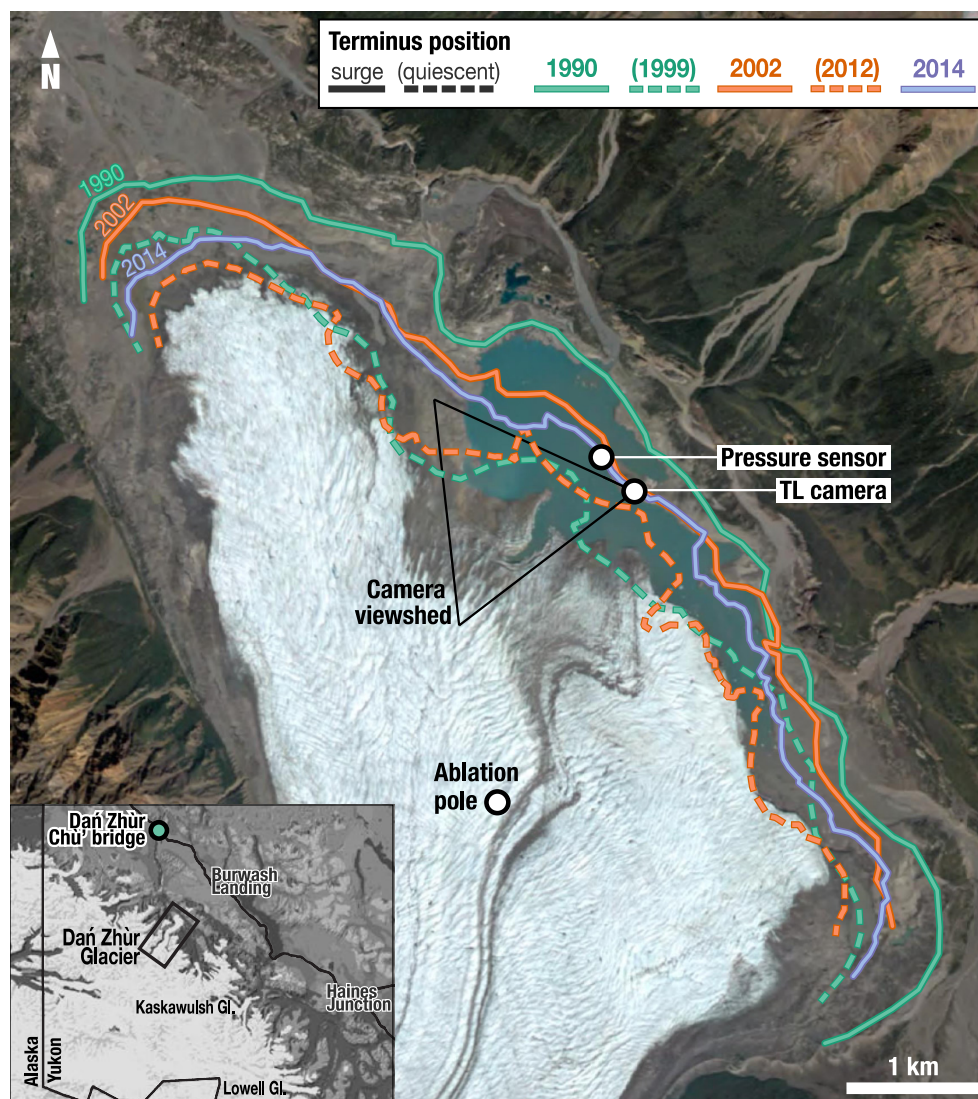
We used field, airborne, and satellite remote sensing observations to determine the causes, patterns, and mechanisms of the drainage of Dañ Zhùr Lake over the last three surge cycles since 1988, with a particular focus on events since the termination of the most recent surge in 2014. We use these data to examine temporal changes in glacier and lake extent and volume, and their connection to glacier surging, along with the causes and routing of past lake drainage events and how they are changing in a warming climate.

3.1. Satellite imagery

For the three surge-quiescent periods since 1988, we acquired satellite scenes from Landsat 5, 7, and 8 (15–30 m resolution), ASTER (15 m), Sentinel-2A (10 m), and Planet (3–5 m). The imagery was preferentially acquired during snow-free months (May–September) and during periods of lake formation and drainage. The Planet images were sourced from <https://planet.com> under their Education and Research Program (Planet Team 2017), while all others were sourced from the United States Geological Survey Earth Explorer (<https://earthexplorer.usgs.gov>). The terminus position at its maximum surge extent in 1988–1990, 2000–2002, and 2012–2014, and subsequent minimum quiescent extent were mapped in QGIS using Landsat 5, Landsat 7, and Planet imagery (Fig. 1). Planet satellites were the main source for imagery since 2014 due to their higher spatial and temporal resolution than Landsat.

We mapped all of the lake drainage routes using Planet and Landsat imagery for the past three surge-quiescent cycles since 1988 by comparing scenes as close in time as possible, typically within days before and after each drainage event (e.g., Figs. 2 and 3). For most lake drainage events, the routing of the river was clear in after-drainage images, either through, under, or around the glacier terminus. A second in-

Fig. 1. Inset: location of Dañ Zhùr Glacier, southwest Yukon, Canada. Main panel: surge extent (solid lines) and quiescent extent (dashed lines) over the last three surge cycles, and locations of the pressure sensor, timelapse (TL) camera, and ablation pole. Base image: 6 July 2019 (Planet). Projection: WGS84, UTM zone 7N (EPSG: 32607).



dication of drainage location was the gathering of icebergs in one part of the lake prior to drainage, due to currents drawing them to that spot.

The extent of Dañ Zhùr Lake on 7 July 2017, 18 August 2018, and 6 July 2019, derived from Planet images acquired shortly before drainage each year, was manually outlined in QGIS3.4. Lake area was then calculated in QGIS, based on the number of digital elevation model (DEM) pixels within each lake outline (see next section for DEM details). We assume that the lakebed remained stable between these dates due to limited time for erosional processes.

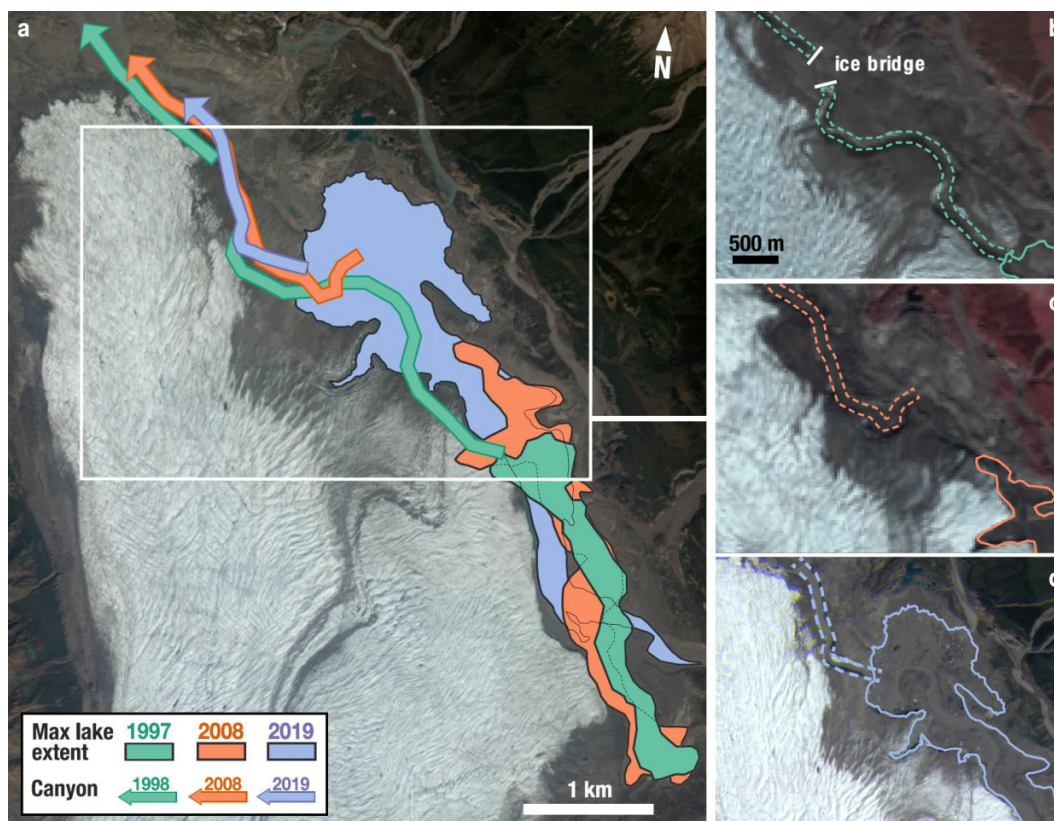
3.2. Airborne measurements

Before and after the most recent drainage event of Dañ Zhùr Lake in summer 2019, we undertook aerial photogrammetry surveys across the glacier to create orthomosaics and DEMs. We surveyed lakebed and downstream areas on 30 June 2019 (437 photos, prior to lake drainage) and 6 Septem-

ber 2019 (533 photos, after lake drainage). These surveys used a Nikon D850 45-megapixel camera with a 24 mm lens, which captured nadir photographs every 3 s. We took the photographs through a port in the underside of a Helio Courier aircraft operated from Silver City Airfield, 60 km southeast of Dañ Zhùr Glacier. Global navigation satellite system (GNSS) observations were recorded at 10 Hz with a Trimble R7 dual frequency global positioning system receiver and an Antcom antenna (model 42GNSSA-XT-1). The positions of the photographs were recorded by using an electrical impulse triggered by the camera flash mount to place a marker in the GNSS record.

We processed the GNSS data collected during each survey with the Precise Point Positioning service of Natural Resources Canada (<https://webapp.geod.nrcan.gc.ca/geod/tools-outils/ppp.php>), which enables reconstruction of the position of the GNSS antenna to an accuracy of up to a decimeter or less from precise orbital information that is released ap-

Fig. 2. (a) Maximum lake extent at Dañ Zhùr Glacier during each quiescent period (25 September 1997, 27 June 2008, and 6 July 2019), and location of subaerial ice canyons that formed after each lake drainage event. Base image: 30 June 2019 (Planet). White box indicates extent of (b), (c), and (d), showing the ice canyon on (b) 28 September 1998 (Landsat 5), (c) 15 August 2008 (Landsat 5), and (d) 26 July 2019 (Planet). Projection: WGS84, UTM zone 7N (EPSG: 32607).



proximately 12 days after data acquisition. We then used a custom Python script (available at <https://github.com/willkochtitzky/photostodem>), which uses a linear interpolation between known locations, to find the position of the photograph relative to a given event marker in the GNSS record.

The photographs captured during the aerial photo surveys were loaded into Agisoft Metashape Professional version 1.6.3, together with their location determined from the GNSS observations. After inspection, any unnecessary images were deleted, such as photographs where the aircraft was turning and photographs from locations outside the area of interest. We then processed the remaining photographs and their positions to produce a sparse point cloud, which is a 3D representation of the tie-point data, involving feature detection and matching procedures (Agisoft 2020). We then exported DEMs with a resolution of 2 m, and orthomosaics with a resolution of 0.5 m. We co-registered the DEMs by minimizing vertical displacement over stable ground using a Python script from Shean et al. (2016).

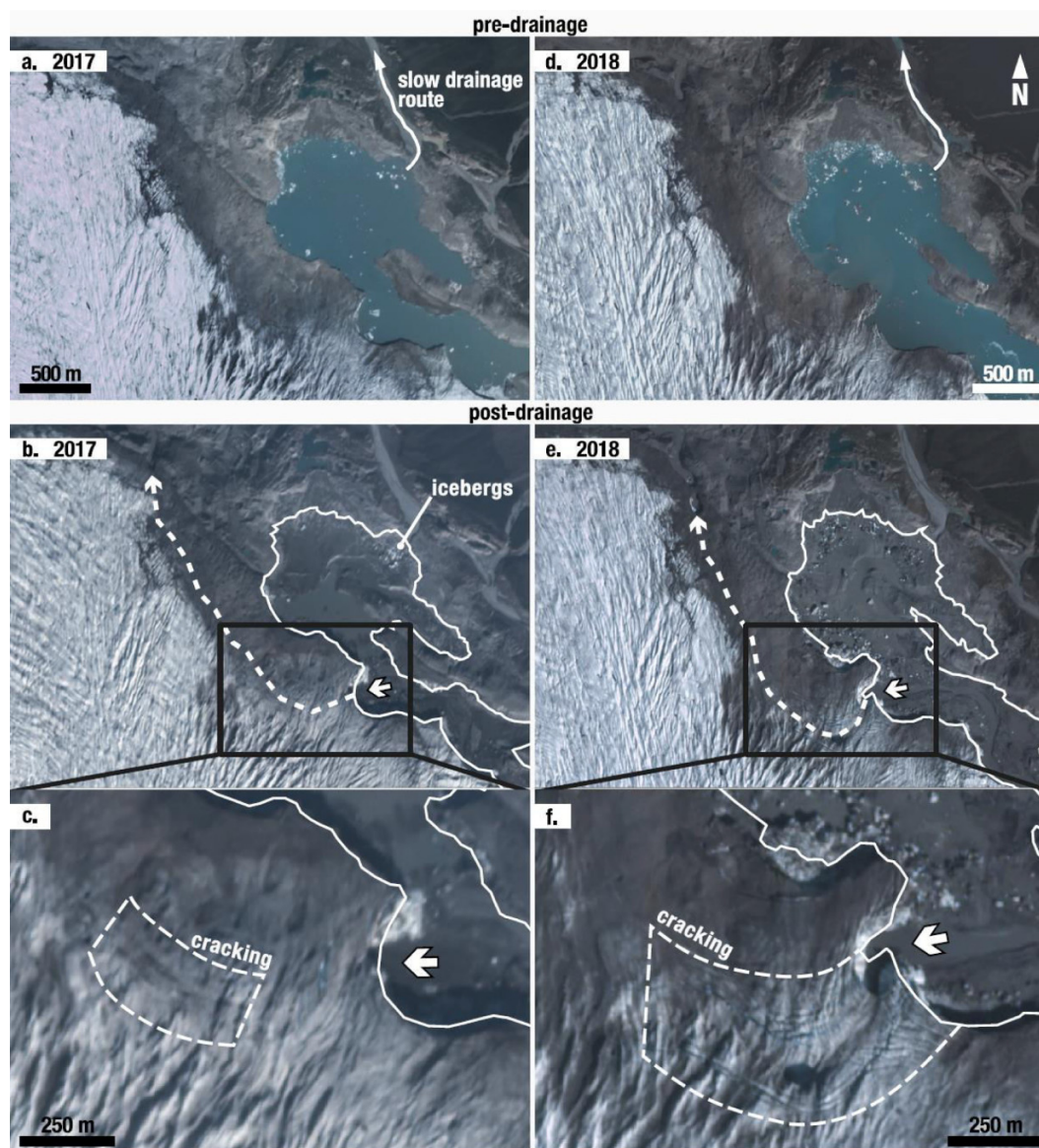
The lake volume was calculated in ArcMap 10.6.1 using the 2019 DEMs and lake area derived from satellite images and air photos taken in 2017, 2018, and 2019. The lake level in each year was set to 1090 m a.s.l., as this is the elevation of a river that flows through a bedrock outlet at the northeast end of the lake (“slow drainage route” in Fig. 3a), which limits the maximum elevation that the lake can reach. This lake sur-

face elevation was compared to the 6 September 2019 DEM of the lakebed, which was cropped to the extent of the lake before it drained in each respective year. Once these steps were complete, the resulting datasets included both a lake surface elevation value and a lakebed DEM for the respective year. With these values, we calculated the lake volume for 2017, 2018, and 2019 in ArcMap using the surface volume tool.

3.3. Field measurements

We installed an Onset HOBO U20-001-01 water level pressure logger near the edge of Dañ Zhùr Lake on 12 July 2019, which captured the drainage event that summer (Fig. 1). The logger was placed on the lake bed in a water depth of approximately 8 m, although due to safety constraints and not already having a map of lake bathymetry, this was not the deepest part of the lake, which reached >50 m in places. Absolute pressure measurements were taken every 30 min and converted to water head assuming water density of 1000 kg m^{-3} , with the logger having a typical error of $\pm 0.05 \text{ cm}$ for water level. The pressure logger data were used to determine a rate of water depth change by subtracting each value from the value recorded 30 min previously. The pressure logger was settled on a ledge above the bottom of the lake, so captured the onset of the 2019 drainage until it was exposed

Fig. 3. (a, b, and c) Extent and drainage routes of Dañ Zhùr Lake before and after the 2017 drainage event, and (d, e, and f) 2018 drainage event. Solid white outlines indicate full lake extent for that year, thick white arrows show inlet and outlet of subglacial channel, and dashed white outlines indicate intense crevassing above subglacial channel. Slow drainage route refers to river outflow over bedrock, which occurs at an elevation of 1090 m a.s.l. when lake is full. Black box indicates extent of (c) and (f). Base images from Planet: (a) 7 August 2017; (b and c) 1 October 2017; (d) 18 August 2018; and (e and f) 30 August 2018. Projection: WGS84, UTM zone 7N (EPSG: 32607).



around 12:00 local time (Pacific Standard Time (PST)) on 13 July 2019. Using the water depth change during this time, along with the September 2019 DEM, we calculated the lake drainage rate and volume change while the transducer was submerged.

We also captured the 2019 drainage event using a SpyPoint solar trail camera, which was installed on 12 July 2019 on a small tripod securely mounted on bedrock, and recorded images hourly. The camera overlooked the lake and terminus of Dañ Zhùr Glacier (Figs. 1 and 4), including the location where the lake drained.

An ablation pole was drilled into the ice on the lower terminus of Dañ Zhùr Glacier on 12 July 2019 (Fig. 1). Ablation rates

were determined from the melting out of stripes marked on the pole every 5 cm with coloured tape, as recorded in hourly photos from a SpyPoint solar trail camera pointed at the pole.

3.4. Flotation calculations

We determined which areas of the glacier terminus were likely to float at the maximum lake depth in 2019 based on the difference in density between ice (917 kg m^{-3} ; Shumskiy 1960) and water (1000 kg m^{-3}), with flotation assumed to occur when lake depth exceeds 0.917 times the ice thickness. We used the 2019 DEMs to extract elevation values for the glacier surface, lake surface (June 2019 DEM), and empty lakebed (September 2019 DEM). We then calculated ice thick-

Fig. 4. Images from the timelapse camera (see viewed in Fig. 1) showing before, during, and after 2019 lake drainage: (a) July 12, 15:30; (b) July 13, 23:30; and (c) July 15, 17:30. All times are in local Pacific Standard Time (PST) (GMT-8). For scale, it is approximately 1 km from the camera to the edge of the glacier.



ness by subtracting the ice elevation at the top of the calving face with the lakebed elevation at the bottom of the calving face. We also calculated the water level by subtracting the lakebed elevation from the lake surface elevation along the calving face. Some uncertainty in the flotation calculation occurs due to use of the density value for pure ice, given that density can vary depending on factors such as crevassing and

the mass of debris within the ice. However, its effect is likely minor given the large changes in lake depth that occurred.

4. Results

4.1. Drainage events since 1988–1990 surge

After the 1988–1990 surge event, several small lakes formed at the glacier terminus between 1991 and 1993, each less than 0.1 km^2 in area. A larger lake began to develop in a basin at the southeast side of the terminus in 1994, which gradually expanded to reach 0.65 km^2 by 1996 (Kochtitzky et al. 2020). Subsequently, a new lake formed to the north of the terminus, and then drained into the lake that was already present, creating an even larger southern lake with an area of $\sim 0.9 \text{ km}^2$ in August 1997 (Fig. 2). In fall 1997, a portion of this lake drained, reducing its area to 0.32 km^2 . In spring 1998, the remainder of the lake drained through a subglacial channel, which eventually collapsed to form a subaerial ice canyon through the entire thickness of the glacier terminus (Fig. 2b), preventing the lake from forming again until after the next surge event.

4.2. Drainage events since 2000–2002 surge

The next surge started in winter 2000 and ended in fall 2002, resulting in the formation of several small lakes at the terminus as the advancing glacier began to block Dañ Zhùr Chù. By September 2002, another lake began to form, which grew to an area of 0.68 km^2 (Kochtitzky et al. 2020). The lakes grew to reach about 1.17 km^2 in summer 2003, and then persisted through 2004 and 2005, with some small fluctuations in size. By 23 June 2006, there was a northern lake and a southern lake that together totalled 1.12 km^2 in area, but by the end of that month it appears they drained subglacially through the glacier terminus, close to where the ice canyon formed during the 1998 drainage. This channel closed during the following winter of 2006 and 2007, and both the southern and northern lakes began to reform. The northern lake drained before the end of summer 2007, but the southern lake persisted until summer 2008 (Fig. 2), when a subaerial ice canyon was formed through the terminus (Fig. 2c), which prevented any further lakes from forming until after the next surge.

4.3. Drainage events since 2012–2014 surge

After the 2012–2014 surge event, the largest lake in at least the past century formed. In 2017, the lake drained subglacially but left a small lake behind (Figs. 3a and 3b). The subglacial drainage channel caused a depression in the overlying ice, leading to cracking and crevassing on the surface (Fig. 3c). The subglacial channel closed that winter, causing the lake to reform, and in August 2018, the lake drained again, through the same subglacial channel as used during the 2017 drainage event (Figs. 3d and 3e). The August 2018 drainage resulted in the roof of the now larger subglacial channel to further subside. This subsidence made it more pronounced on the glacier surface, and was accompanied by a larger area of surface crevassing that followed the route of the subglacial channel (Fig. 3f). Dañ Zhùr Chù then flowed through this subglacial

channel during the remainder of 2018, as it had done in late 2017, until the channel closed again that winter.

4.3.1. 2019 drainage event

The timelapse camera and pressure transducer provide a detailed timeline of lake levels during the 2019 lake drainage event (Figs. 4 and 5). These instruments show that drainage started at 17:30 PST on 12 July 2019 and continued until about noon on 15 July 2019.

The pressure logger recorded an initial lake level change rate of less than -0.10 m h^{-1} from 17:30 PST until 23:30 PST on 12 July, after which the lake began to drain faster (Fig. 5a). The lowering rate continued to accelerate until $\sim 09:30$ PST on 13 July when there was a reduction in the rate of change until 11:00. Lake drainage then accelerated rapidly to reach a peak lake level change of -1.76 m h^{-1} at 12:00, equating to a drainage rate of almost $200 \text{ m}^3 \text{ s}^{-1}$ (Fig. 5b). Soon thereafter the sensor was exposed to the atmosphere, but the lake continued to drain as the transducer was not at the bottom of the lake. The timelapse camera shows that the lake was completely drained by 12:00 PST on 15 July 2019.

The location of the 2019 drainage differed from that in 2017 and 2018. Although the prominent subglacial channel where the previous two drainage events occurred is visible in the satellite imagery (Fig. 6), the water did not drain through the same route in 2019. Instead, a new channel developed under the ice at the north end of the lake, very close to the boundary between the glacier terminus and adjacent bedrock. The channel first developed subglacially, with the roof eventually collapsing to form a subaerial ice canyon, which extended through the entire thickness of the glacier terminus. This new channel cut through the terminus to connect with the downstream portion of the old drainage channel (Fig. 6b).

Satellite imagery and the timelapse camera show that on 16 July 2019, the roof of the new channel was still present. On 18 July, some subsidence and collapse of the roof occurred near the channel entrance (Figs. 7a and 7b), as indicated by expanding crevasses on either side. The canyon continued to grow over the following days (Figs. 7c, 7d, and 7e), until the roof completely collapsed on 23 July (Fig. 7f).

To better understand the mechanisms that could cause drainage, we calculated the likelihood of flotation at the terminus of Dañ Zhùr Glacier when the lake was at its maximum level in July 2019, just prior to the drainage (Fig. 6b). Two areas at the glacier terminus are most likely to float: the northwest corner of the lake, where the 2019 canyon formed, and to the east of the 2017 and 2018 drainage outlet. At the northwest site the ice cliff was $\sim 68 \text{ m}$ high, while the mean lake depth at that location was $\sim 56 \text{ m}$. At the eastern site the ice cliff was $\sim 40 \text{ m}$ high, while the mean water depth was $\sim 32 \text{ m}$.

4.4. Lake area and volume changes

Lake area and volume, calculated using our September 2019 DEM and satellite imagery from 7 July 2017, 18 August 2018, and 6 July 2019 (when the lake was close to its annual maximum extent), both increased in size each year between

2017 and 2019, with the greatest increase between 2018 and 2019 (Fig. 8). Between 2017 and 2018, the lake area grew from 1.49 to 1.90 km^2 and reached its maximum extent of 2.45 km^2 in 2019. During the same period, the lake volume increased from 0.0361 km^3 in 2017 to 0.0493 km^3 in 2018, and reached a maximum of 0.0603 km^3 in 2019.

5. Discussion

5.1. Mechanism of Dañ Zhùr Lake drainage events

Satellite imagery indicates several similarities in the drainage mechanisms that occurred during each quiescent period, with all drainage events first occurring subglacially through a channel under the terminus of the glacier. During the first two or three drainage events of each quiescent period the roof of the subglacial channel remained intact, but in the final drainage of each period the roof collapsed to form a canyon through the entire glacier thickness, thus preventing future lake formation until the next surge and associated advance of the glacier (Fig. 2).

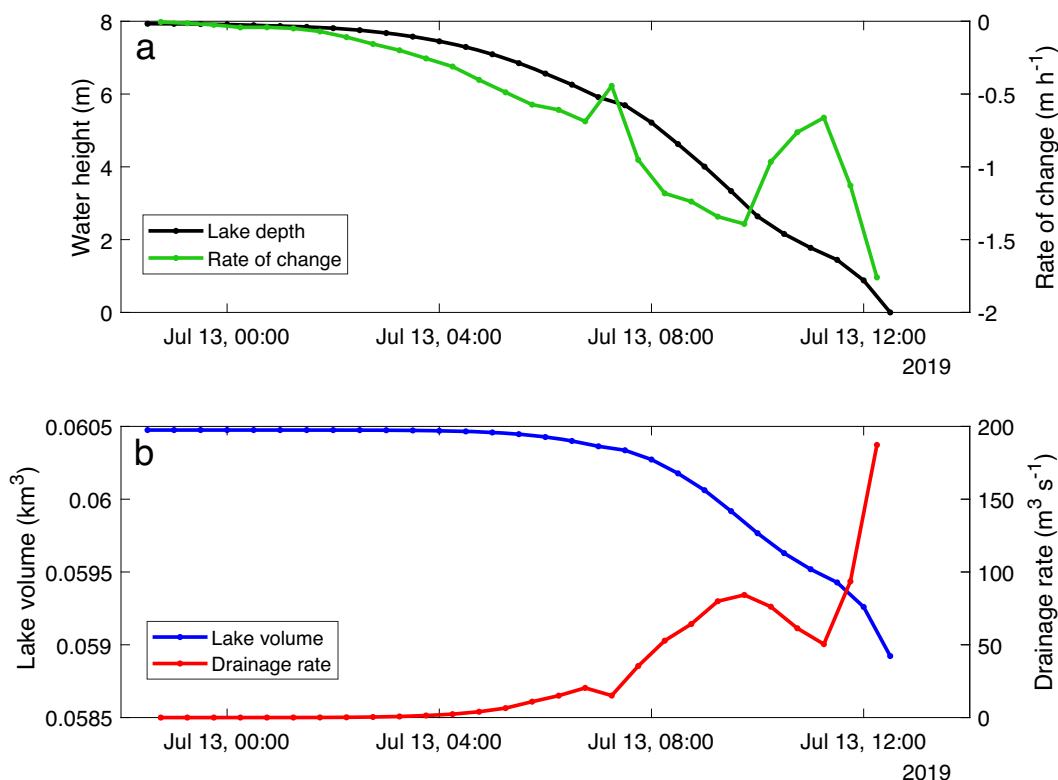
During a surge, there is sufficient deformation of the ice to close the ice canyon and any previous subglacial channels over a matter of months. For example, the maximum velocity of the terminus of Dañ Zhùr Glacier during the 2012–2014 surge was 1150 m year^{-1} (Kochtitzky et al. 2019), so final ice canyon widths of $\sim 100\text{--}400 \text{ m}$ over the previous three quiescent phases would have taken approximately 1–4 months to completely close once the next surge began. The ability of Dañ Zhùr Glacier to advance and close these channels during future surges will dictate whether future lakes are able to form at the terminus.

Subglacial channels within a single quiescent period did not always occur in the same location, as exemplified by the difference in location of the channels in 2017/2018 versus 2019 (Fig. 6b). However, the location of the final drainage channel in each quiescent period, which becomes subaerial, has been in a nearly identical location for each of the past three periods (Fig. 2). The location of this final drainage channel is near where the glacier pushes up against a bedrock cliff, and in 2019 was one of the locations where ice surface elevations were lowest (elevation data are unavailable for earlier periods).

5.2. 2017–2019 drainage events

Only the lower portion of the subglacial channel from the 2017 and 2018 drainage events was reoccupied during the 2019 drainage (Fig. 6b). The 2019 lake was the largest observed since at least the 1930s, measuring 2.45 km^2 on 6 July 2019 (Kochtitzky et al. 2020). The 2019 drainage channel formed further north than the 2017/2018 channel, close to the northern margin of the glacier. The location of the 2019 channel occurred in one of the thinnest and lowest elevation areas along the terminus, making it the first region to approach flotation when the lake was at maximum depth (Fig. 6a). The 2019 channel also occupied the most direct path from the lake to the lower elevation areas downstream of the glacier terminus.

Fig. 5. (a) Pressure transducer record showing water depth and hourly rate of change at the start of the drainage of Dañ Zhùr Lake, 13 July 2019. (b) Volume and drainage rate of Dañ Zhùr Lake, computed from the pressure transducer record and the empty lake DEM from September 2019. All times are local PST (GMT-8).



Based on the rapid drainage of the entire lake shortly after reaching maximum depth, and potentially flotation, we can make some inferences about the processes that must have occurred at the glacier bed. In a stable situation, it might be expected that the glacier terminus would stop floating as the water level drops in the adjacent lake, resulting in the shutting down of the subglacial outflow (Liestøl 1956; Björnsson 2010). However, the continued drainage of Dañ Zhùr Lake during each event indicates that channel volume growth occurred faster than ice deformation could close it, due to frictional heating from drainage of the lake water, providing an efficient conduit for continued water discharge (Nye 1976; Clarke 1982).

The highest lake level is controlled by the elevation of the northeast bedrock outlet at ~1090 m a.s.l. (Fig. 3a). This outlet does not, however, limit the maximum area of the lake because as the glacier retreats, it exposes a larger, and potentially deeper, lake basin. This increase in available basin size explains why Dañ Zhùr Lake has been getting larger toward the present day (Figs. 1 and 8).

The full lake drainage took ~66.5 h between the evening of 12 July and mid-day on 15 July. Based on our calculations from the pressure transducer and the September 2019 DEM, the lake drainage rate increased to 84 m³ s⁻¹ ~10 h after the main drainage began (i.e., around 09.30 on 13 July; Fig. 5b). The drainage rate then dropped to 50 m³ s⁻¹ over a period of 1.5 h, before rapidly increasing to a maximum of 187 m³ s⁻¹ until the pressure transducer was exposed. Over this period,

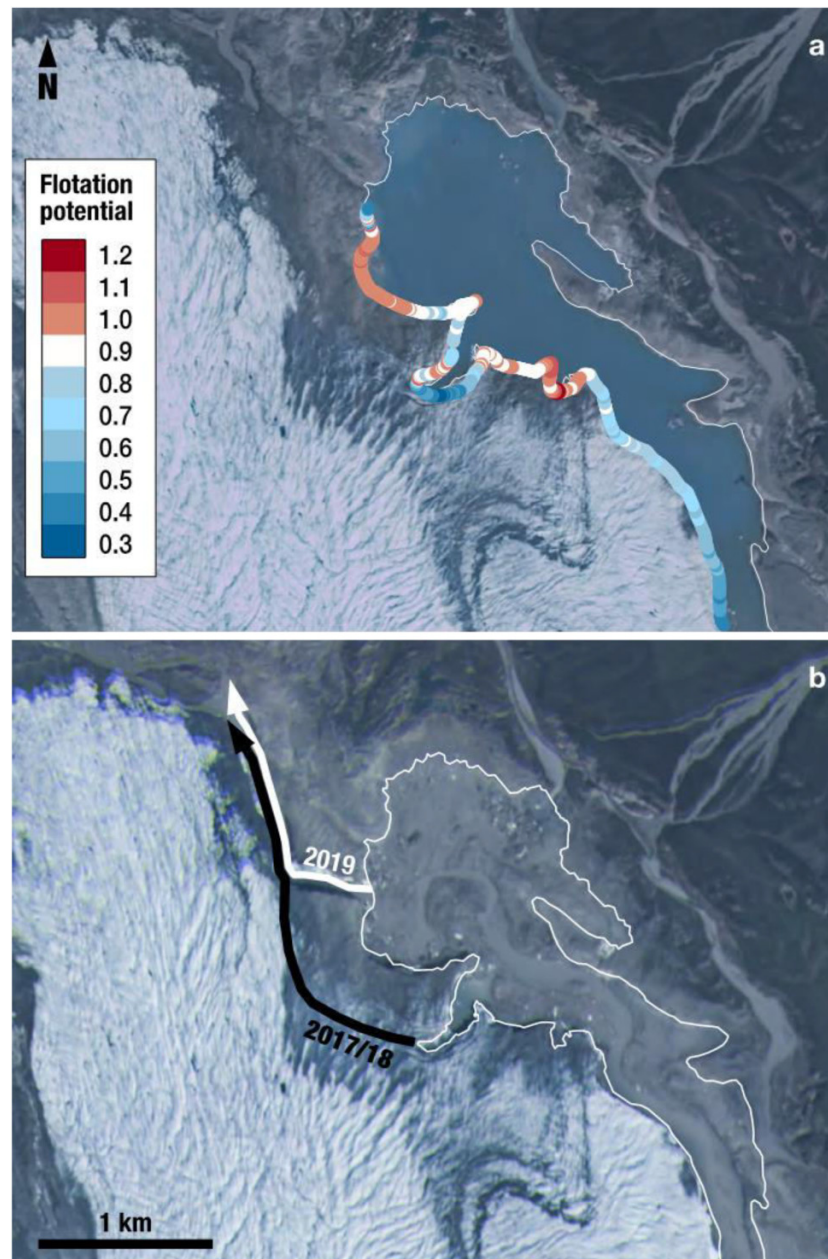
0.0016 km³ (16 000 000 m³) of lake volume was drained downstream (Fig. 5b). The reduction in drainage rate during this period may be linked to growth of the subglacial channel and (or) change in the efficiency of the subglacial flow as the lake level dropped back to below ice flotation level. We are unable to calculate the temporal change in drainage rate once the pressure transducer was exposed, but based on a remaining drainage time of 47.5 h and remaining lake volume of 0.0589 km³, the average drainage rate for the rest of lake emptying was ~345 m³ s⁻¹.

5.3. Implications of flooding downstream

One of the main concerns about GLOFs around the world is downstream hazards as water drains rapidly from the lake (Haerberli and Whiteman 2015; Hock et al. 2019). Modelling undertaken by Clarke and Mathews (1981) suggested that a large lake caused by a full blockage of Dañ Zhùr valley could lead to significant damage to downstream infrastructure if it were to rapidly drain, but a full blockage of the valley is very unlikely to occur today due to the overall retreat of the glacier since the 1930s (Kochtitzky et al. 2019). In the case of recent drainages of Dañ Zhùr Lake, the main potential risks are to recreational users of the area and the Alaska Highway bridge that crosses Dañ Zhùr Chù' about 50 km downstream of the terminus.

The area on the eastern bank downstream of Dañ Zhùr Glacier is frequented by hikers and pack rafters, with an av-

Fig. 6. Drainage routes at the terminus of Dañ Zhùr Glacier before (a) and after (b) 2019 drainage event in Planet imagery. (a) 30 June 2019, white outline indicates full lake extent, colours show flotation potential, red is most likely (>1), blue is least likely (<1). (b) July 26, 2019, white outline indicates full lake extent from (a), arrows show location of ice canyons where lake drained in 2017 and 2018 (black), and 2019 (white). Projection: WGS84, UTM zone 7N (EPSG: 32607).



erage of 72 visitors per year between 2017 and 2021 (pers. comm., Carmen Wong, Parks Canada, 2023). The Dañ Zhùr hiking route includes a section ~15 km long, which passes near the glacier, and for a section ~6 km long from the bottom of Hoge Creek to the glacier terminus, there is a risk of flooding during a rapid drainage of Dañ Zhùr Lake. While there is no defined trail, Parks Canada recommends hiking in the valley bottom, alongside the river, if possible. On 15 July 2019, just a day after the lake had finished draining, a hiker reported large volumes of wet mud deposited in trees between Hoge Creek and the terminus of the glacier, with some small streams of water running through the vegetation

(CBC 2019). This mud was likely deposited by flooding due to the lake drainage and demonstrates the potential hazard to recreational users if they hike or camp near the river during an outburst flood.

The Alaska Highway Bridge, ~50 km downstream of Dañ Zhùr Glacier, was most recently replaced in 2007 and is about 270 m long and intended to last 75 years (Whitehorse Daily Star 2007). While this is the only known permanent infrastructure in the path of outburst floods from Dañ Zhùr Glacier, this area also includes traditional hunting grounds of members of Kluane First Nation, who sometimes erect seasonal infrastructure. The bridge is part of the primary access route

Fig. 7. Timelapse camera photos of the development of the ice canyon at the terminus after the 2019 drainage event. Red box indicates canyon location. All times are local PST (GMT-8).



between the US and Yukon, and sees a lot of local, tourist, and commercial travel, especially during the summer months when outburst floods occur. However, previous floods have not caused any known damage to the bridge, and no hydrographic stations exist nearby to monitor how the water levels changed here during past outburst floods.

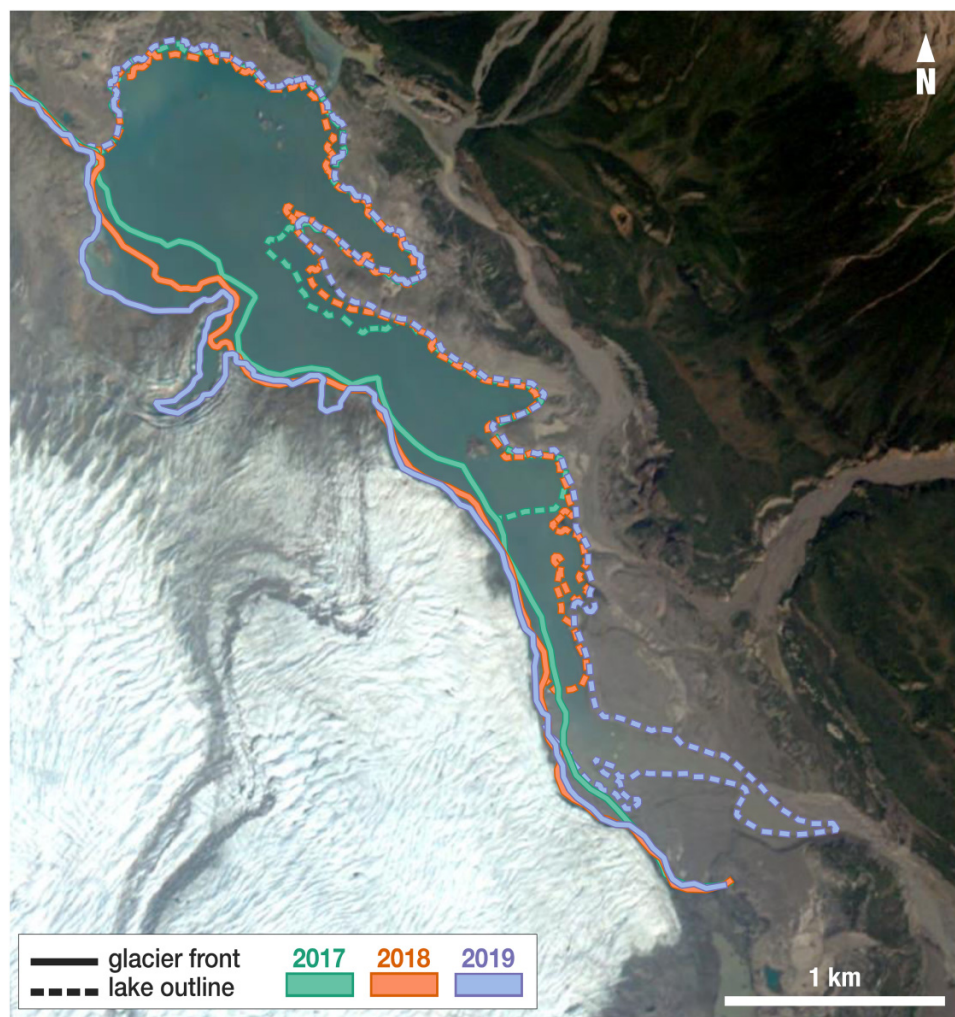
5.4. Future evolution of GLOFs at Dañ Zhùr Glacier

Before the next surge of Dañ Zhùr Glacier, which can be expected to begin in the mid-2020s if past surge cycle trends continue, there is little to no risk of a GLOF as it is highly unlikely that the lake will form due to the size of the ice canyon created in 2019 (Fig. 2d), and which continues to exist today

(summer 2022). After the next surge, and potentially for the next few decades, an ice-dammed lake is likely to form again as the advancing glacier terminus blocks Dañ Zhùr Chù', as it has done during the previous three surge events. During this next quiescent phase, it is possible that larger lakes will occur than in 2017, 2018, and 2019, due to the increasing size of the basin at the terminus of the glacier as the ice continues to recede.

In the long term, it is likely that the risk of GLOFs at Dañ Zhùr Glacier will ultimately disappear as the glacier continues to recede, as every surge event reaches a less advanced extent than the previous one. Eventually, one of these surges will not extend far enough into the valley to dam Dañ Zhùr Chù', and no ice-dammed lake will form. This long-term reduction in ice extent is similar to what occurred at Nàhùdäy

Fig. 8. Dañ Zhùr lake extent (dashed lines) and terminus positions (solid lines) for 2017, 2018, and 2019. Base image: 30 June 2019 (Planet). Projection: WGS84, UTM zone 7N (EPSG: 32607).



Glacier, which dammed the Alesk River multiple times during the 19th century and before (Clague and Rampton 1982), but has not blocked it over at least the past century as each recent surge of Nàlùdäy has been less extensive than the previous (Bevington and Copland 2014). It is not possible to provide a precise prediction for when surges of Dañ Zhùr Glacier will no longer block Dañ Zhùr Chù', but it will likely be at least several decades from now. Future work to better map the bedrock elevation beneath the glacier terminus would help illuminate if and how Dañ Zhùr Glacier could dam the river in the future.

6. Conclusions

Surges of Dañ Zhùr Glacier result in the blockage of Dañ Zhùr Chù' and the associated formation of a large ice-dammed lake. We document that the growth of channels through the ice after the past three surge events played a key role in drainage of the lake. We also show that the first drainage event after a surge does not occupy the same channel as the final drainage event of each quiescent phase,

demonstrating evolution of the drainage mechanisms influenced by ice terminus thickness and relative lake depth as the glacier retreats. The last lake to form after each surge cycle resulted in an ice canyon that first forms subglacially and is then exposed subaerially, which prevents lake formation until the next surge advance. The 2019 drainage event was the largest on record, with air photo derived DEMs indicating a total lake volume of 0.0603 km^3 . This lake took $\sim 66.5 \text{ h}$ to fully drain, with a mean discharge rate of $\sim 345 \text{ m}^3 \text{ s}^{-1}$ for the final 47.5 h.

In the short term (after the next surge cycle, and potentially up to a few decades from now), it is possible that the ice-dammed lake, and associated floods, will be larger due to the increasingly large basin created by glacier recession. However, in the longer term, lake formation is likely to cease altogether due to the changing geometry of the glacier terminus, as each surge is causing a smaller advance of the glacier than the previous one, resulting in a reduced ability to block Dañ Zhùr Chù'. Because the draining and filling of this lake is semi-predictable, future research in this area could enhance our understanding of ice-dammed lake and subglacial pro-

cesses, which are important in keeping communities around the world safe from GLOFs.

The floods caused by drainage events from Dañ Zhùr Lake are a potential risk to people and infrastructure downstream. The area close to the glacier is frequented by hikers and pack rafters who could be on or nearby Dañ Zhùr Chù' at the time of a drainage event. During the next surge and subsequent quiescent phase, it would be beneficial to monitor the size of the ice-dammed lake and thickness of the glacier terminus to help predict the drainage event. Regular monitoring of satellite imagery and associated glacier velocity mapping should also occur to enable detection of the next surge of Dañ Zhùr Glacier. Having this information would diminish the risk to recreational users in downstream areas of Dañ Zhùr Chù'.

Acknowledgements

Fieldwork for this project was conducted on Kluane First Nation Traditional Territory, and the authors thank the community for permission to work there, and particularly Kate Ballegooyen and Rachael Thom for their communication. The authors thank Parks Canada, and particularly Carmen Wong, for their interest and support throughout this project, with field measurements completed under Parks Canada Research and Collection Permit KLU-2019-31740. The authors thank the staff at Kluane Lake Research Station, and pilots from Icefield Discovery and Trans North helicopters for their support in the field.

Article information

History dates

Received: 5 January 2023

Accepted: 4 May 2023

Accepted manuscript online: 23 May 2023

Version of record online: 16 June 2023

Notes

Luke Copland served as Associate Editor at the time of manuscript review and acceptance; peer review and editorial decisions regarding this manuscript were handled by Remi Amiraux.

Copyright

© 2023 The Author(s). This work is licensed under a [Creative Commons Attribution 4.0 International License](https://creativecommons.org/licenses/by/4.0/) (CC BY 4.0), which permits unrestricted use, distribution, and reproduction in any medium, provided the original author(s) and source are credited.

Data availability

All satellite imagery used in this study is publicly available from data sources listed in the methods. The DEMs, orthomosaics, timelapse camera images, water pressure records, and GNSS data generated and collected for this study are available by contacting LC (luke.copland@uottawa.ca).

Author information

Author ORCIDiDs

Luke Copland <https://orcid.org/0000-0001-5374-2145>

Christine Dow <https://orcid.org/0000-0003-1346-2258>

Will Kochtitzky <https://orcid.org/0000-0001-9487-1509>

Dorota Medrzycka <https://orcid.org/0000-0002-5391-3239>

Author contributions

Conceptualization: MP, LC, CD

Data curation: LC

Formal analysis: MP, CD, WK, DM

Funding acquisition: MP, LC, CD

Investigation: MP, LC, CD, WK, DM

Methodology: MP, LC, CD, WK, DM

Project administration: LC, CD

Resources: LC, CD

Software: WK, DM

Supervision: LC, CD

Visualization: MP, WK, DM

Writing – original draft: MP, LC, CD, WK, DM

Writing – review and editing: MP, LC, CD, WK, DM

Competing interests

The authors declare there are no competing interests.

Funding information

Financial and logistical support for this work was provided by the University of Ottawa, University of Waterloo, Northern Scientific Training Program, W. Garfield Weston Foundation, Canada Foundation for Innovation, Ontario Research Fund, New Frontiers in Research Fund, Canada Research Chairs Programme, Association of Canadian Universities for Northern Studies, Yukon Government, Yukon Foundation Scholarships, Natural Sciences and Engineering Research Council of Canada, Planet Education and Research Program, and Polar Continental Shelf Program.

References

- Abe, T., Furuya, M., and Sakakibara, D. 2016. Brief communication: twelve-year cyclic surging episodes at Donjek Glacier in Yukon, Canada. *The Cryosphere*, 10(4): 1427–1432. doi:[10.5194/tc-10-1427-2016](https://doi.org/10.5194/tc-10-1427-2016).
- Agisoft, L.L.C. 2020. Agisoft Metashape user manual, Professional edition, Version 1.6. Agisoft LLC, St. Petersburg, Russia. Available from https://www.agisoft.com/pdf/metashape-pro_1_6_en.pdf [accessed March 2020].
- Bevington, A., and Copland, L. 2014. Characteristics of the last five surges of Lowell Glacier, Yukon, Canada, since 1948. *Journal of Glaciology*, 60(219): 113–123. doi:[10.3189/2014JG13J134](https://doi.org/10.3189/2014JG13J134).
- Björnsson, H. 1992. Jökulhlaups in Iceland: prediction, characteristics and simulation. *Annals of Glaciology*, 16: 95–106. doi:[10.3189/1992AoG16-1-95-106](https://doi.org/10.3189/1992AoG16-1-95-106).
- Björnsson, H. 2009. Jökulhlaups in Iceland: sources, release and drainage. *In* Megaflooding on Earth and Mars. Edited by D.M. Burr, P.A. Carling and V.R. Baker. Cambridge University Press, Cambridge, UK. pp. 50–64. doi:[10.1017/CBO9780511635632.004](https://doi.org/10.1017/CBO9780511635632.004).
- Björnsson, H. 2010. Understanding jökulhlaups: from tale to theory. *Journal of Glaciology*, 56(200): 1002–1010. doi:[10.3189/002214311796406086](https://doi.org/10.3189/002214311796406086).
- CBC. 2019. 'Super lucky to catch it': researchers get time-lapse video of glacial lake flood [online]. Available from <https://www.cbc.ca/news/ca>

- nada/north/glacial-lake-bursts-in-yukon-1.5312116 [accessed 9 October 2019].
- Clague, J.J., and Rampton, V.N. 1982. Neoglacial Lake Alesk. *Canadian Journal of Earth Sciences*, **19**(1): 94–117. doi:10.1139/e82-008.
- Clague, J.J., and O'Connor, J.E. 2015. Glacier-related outburst floods. In *Snow and ice-related hazards, risks and disasters*. 2nd ed. Edited by W. Haerberli, C. and Whiteman. Elsevier, Amsterdam, The Netherlands. pp. 467–499. doi:10.1016/B978-0-12-817129-5.00019-6.
- Clarke, G.K.C. 1982. Glacier outburst floods from “Hazard Lake,” Yukon Territory, and the problem of flood magnitude prediction. *Journal of Glaciology*, **28**(98): 3–21. doi:10.3189/S0022143000011746.
- Clarke, G.K.C., and Mathews, W.H. 1981. Estimates of the magnitude of glacier outburst floods from Lake Donjek, Yukon Territory, Canada. *Canadian Journal of Earth Sciences*, **18**(9): 1452–1463. doi:10.1139/e81-136.
- Cruikshank, J. 2001. Glaciers and climate change: perspectives from oral tradition. *Arctic*, **54**(4): 377–393. doi: 10.14430/arctic795.
- Cruikshank, J. 2005. Do glaciers listen? Local knowledge, colonial encounters, and social imagination. UBC Press, Vancouver, BC.
- Haerberli, W., and Whiteman, C. (Editors). 2015. *Snow and ice-related hazards, risks and disasters*. 2nd ed. Elsevier, Amsterdam, The Netherlands. doi:10.1016/C2018-0-00970-6.
- Harrison, S., Kargel, J.S., Huggel, C., Reynolds, J., Shugar, D.H., Betts, R.A., et al. 2018. Climate change and the global pattern of moraine-dammed glacial lake outburst floods. *The Cryosphere*, **12**(4): 1195–1209. doi:10.5194/tc-12-1195-2018.
- Hock, R., Rasul, G., Adler, C., Cáceres, B., Gruber, S., Hirabayashi, Y., et al. 2019. High mountain areas. In *Special Report on the Ocean and Cryosphere in a Changing Climate*. Edited by H.-O. Pörtner, D.C. Roberts, V. Masson-Delmotte, P. Zhai, M. Tignor, E. Poloczanska, et al. Cambridge University Press, Cambridge, UK. pp. 131–202. doi:10.1017/9781009157964.004.
- Iturrizaga, L. 2011. Glacier lake outburst floods. In *Encyclopedia of snow, ice and glaciers*. Edited by V.P. Singh, P. Singh and U.K. Haritashya. Springer, Dordrecht, The Netherlands. pp. 381–399. doi:10.1007/978-90-481-2642-2_196.
- Jóhannesson, T. 2002. The initiation of the 1996 jökulhlaup from Lake Grímsvötn, Vatnajökull, Iceland. *IAHS Publication*, **271**: 57–64.
- Knight, P.G., and Russell, A.J. 1993. Most recent observations of the drainage of an ice-dammed lake at Russell Glacier, West Greenland, and a new hypothesis regarding mechanisms of drainage initiation. *Journal of Glaciology*, **39**(133): 701–703. doi:10.3189/S0022143000016609.
- Kochtitzky, W., Jiskoot, H., Copland, L., Enderlin, E., McNabb, R., Kreutz, K., and Main, B. 2019. Terminus advance, kinematics and mass redistribution during eight surges of Donjek Glacier, St. Elias Range, Canada, 1935 to 2016. *Journal of Glaciology*, **65**(252): 565–579. doi:10.1017/jog.2019.34.
- Kochtitzky, W., Copland, L., Painter, M., and Dow, C. 2020. Draining and filling of ice dammed lakes at the terminus of surge-type Dañ Zhùr (Donjek Glacier), Yukon, Canada. *Canadian Journal of Earth Sciences*, **57**(11): 1337–1348. doi:10.1139/cjes-2019-0233.
- Liestøl, O. 1956. Glacier dammed lakes in Norway. *Norsk Geografisk Tidsskrift*, **15**(3–4): 122–149. doi:10.1080/00291955608542772.
- Maag, H. 1972. Ice-dammed lakes on Axel Heiberg Island, with special reference to the geomorphological effect of the outflowing lake water. In *International Geographical Union Field Tour Ea2: Arctic Archipelago I*. 22nd International Geographical Congress. Axel Heiberg Island Research Reports. Edited by F. Muller. McGill University, Montreal, QC. pp. 39–48.
- Nye, J.F. 1976. Water flow in glaciers: jökulhlaups, tunnels and veins. *Journal of Glaciology*, **17**(76): 181–207. doi:10.3189/S002214300001354X.
- Perchanok, M.S. 1980. History of a glacier-dammed lake on Donjek River, Yukon. Master's thesis, Carleton University, Ottawa, Canada. doi:10.22215/etd/1980-00499.
- Planet Team. 2017. Planet application program interface. In *Space for Life on Earth*. San Francisco, CA. Available from <https://api.planet.com> [accessed April 2023].
- Rick, B., McGrath, D., Armstrong, W., and McCoy, S.W. 2022. Dam type and lake location characterize ice-marginal lake area change in Alaska and NW Canada between 1984 and 2019. *The Cryosphere*, **16**(1): 297–314. doi:10.5194/tc-16-297-2022.
- Sevestre, H., and Benn, D.I. 2015. Climatic and geometric controls on the global distribution of surge-type glaciers: implications for a unifying model of surging. *Journal of Glaciology*, **61**(228): 646–662. doi:10.3189/2015JoG14J136.
- Shean, D.E., Alexandrov, O., Moratto, Z., Smith, B.E., Joughin, I.R., Porter, C.C., and Morin, P.J. 2016. An automated, open-source pipeline for mass production of digital elevation models (DEMs) from very high-resolution commercial stereo satellite imagery. *ISPRS Journal of Photogrammetry and Remote Sensing*, **116**: 101–117. doi:10.1016/j.isprsjprs.2016.03.012.
- Shumskiy, P.A. 1960. Density of glacier ice. *Journal of Glaciology*, **3**(27): 568–573. doi:10.3189/S0022143000023686.
- Somos-Valenzuela, M.A., Chisolm, R.E., Rivas, D.S., Portocarrero, C., and McKinney, D.C. 2016. Modeling a glacial lake outburst flood process chain: the case of Lake Palcacocha and Huaraz, Peru. *Hydrology and Earth System Sciences*, **20**(6): 2519–2543. doi:10.5194/hess-20-2519-2016.
- Taylor, C., Robinson, T.R., Dunning, S., Carr, J.R., and Westoby, M. 2023. Glacial lake outburst floods threaten millions globally. *Nature Communications*, **14**: 487. doi:10.1038/s41467-023-36033-x.
- Walder, J.S., and Costa, J.E. 1996. Outburst floods from glacier-dammed lakes: the effect of mode of lake drainage on flood magnitude. *Earth Surface Processes and Landforms*, **21**(8): 701–723. doi:10.1002/(SICI)1096-9837(199608)21:8<701::AID-ESP615>3.0.CO;2-2.
- Whitehorse Daily Star. 2007. There's a new bridge on the block [online]. Available from <https://www.whitehorsestar.com/News/theres-a-new-bridge-on-the-block> [accessed 9 October 2007].
- Zemp, M., Frey, H., Gärtner-Roer, I., Nussbaumer, S.U., Hoelzle, M., Paul, F., et al. 2015. Historically unprecedented global glacier decline in the early 21st century. *Journal of Glaciology*, **61**(228): 745–762. doi:10.3189/2015JoG15J017.